Science Advances
AAAS

advances.sciencemag.org/cgi/content/full/6/10/eaaz3439/DC1

Supplementary Materials for

Tethered peptide neurotoxins display two blocking mechanisms in the K^+ channel pore as do their untethered analogs

Ruiming Zhao, Hui Dai, Netanel Mendelman, Jordan H. Chill*, Steve A. N. Goldstein*

*Corresponding author. Email: sgoldst2@uci.edu (S.A.N.G.); jordan.chill@biu.ac.il (J.H.C.)

Published 4 March 2020, *Sci. Adv.* **6**, eaaz3439 (2020)
DOI: 10.1126/sciadv.aaz3439

This PDF file includes:

Supplementary Materials

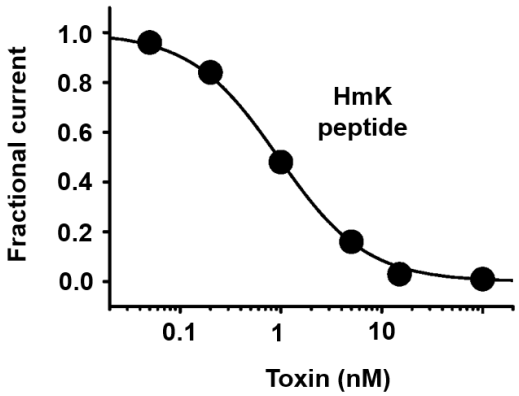

Fig. S1. Concentration-response relationship of HmK blockade of KcsA-Shaker. Inhibition of peptide HmK (●) on KcsA-Shaker was studied by TEVC as described in Materials and Methods and fit to the Hill relationship (Eqn 1). The K_i of peptide HmK for KcsA-Shaker channels was estimated from the fit to be 0.94 ± 0.08 nM with a Hill coefficient of 1.03 ± 0.09. n = 6 for each condition. Values are mean ± SEM. Error bars are smaller than symbols.

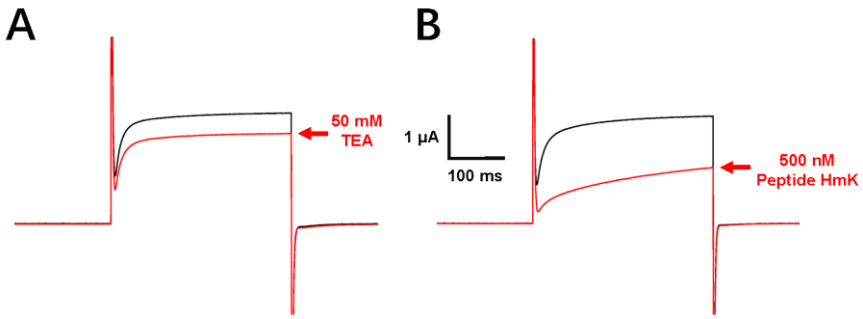

Fig. S2. Effect of mutation KcsA-Shaker–Y82V on block by TEA and HmK. KcsA-Shaker-Y82V were expressed in oocytes and studied by TEVC to assess equilibrium inhibition using a holding voltage of −80 mV, 300 ms test pulses to 0 mV, and a 5 s interpulse interval. **(A)** Representative current trace for KcsA-Shaker-Y82V with 50 mM TEA (red) or without TEA application (black). **(B)** Representative current trace for KcsA-Shaker-Y82V with 500 nM peptide HmK (red) or without peptide application (black).

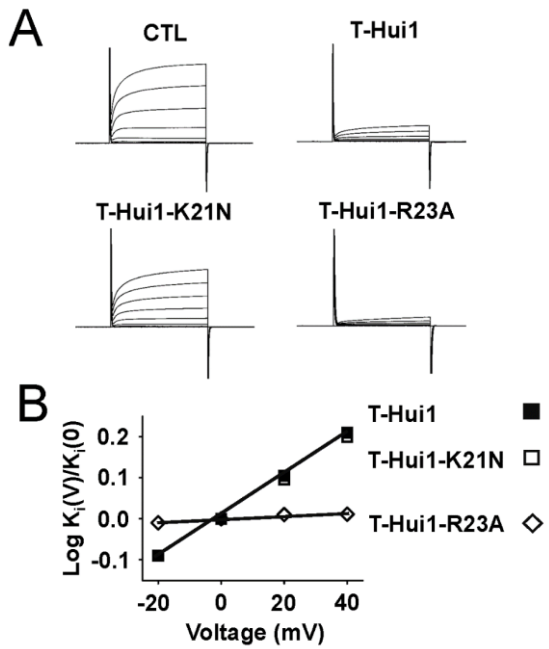

Fig. S3. Hui1-Arg^{23} mediates the voltage-dependent block of KcsA-Shaker. KcsA-Shaker with or without T-Hui1 and variants co-injection were expressed in oocytes and studied by TEVC to assess equilibrium inhibition using a holding voltage of −80 mV, 300 ms test pulses, and a 5 s interpulse interval, n = 18 cells for each condition. Values are mean ± SEM. Some error bars are smaller than symbols. (**A**) Representative current traces (steps of 20 mV from −80 mV to 60 mV) for KcsA-Shaker channels without (CTL), or with co-expression of T-Hui1, T-Hui1-K22N and T-Hui1-R23A after 0.25 ng cRNAs co-injection. (**B**) Effect of voltage on blockade of KcsA-Shaker by T-Hui1 mutants. K_i for T-toxins was determined from -20 mV to 40 mV based on the fraction of unblocked current at equilibrium (F_{un}) and plotted as a ratio to the value at 0 mV.

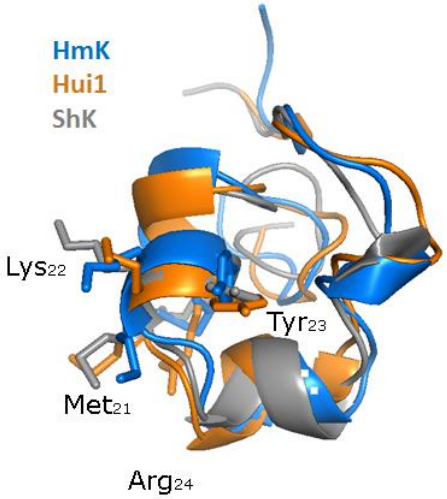

Fig. S4. Structures of HmK, ShK, and Hui1 toxins noting some important, conserved residues. HmK 3D structure adopts a typical SAK1 helix-kink-helix conformation, with residues 14-18 and 22-26 forming two short perpendicular α-helices. Side chains residues Met$_{21}$-Lys$_{22}$-Tyr$_{23}$-Arg$_{24}$ of ShK and HmK (Met$_{20}$-Lys$_{21}$-Tyr$_{22}$-Arg$_{23}$ of Hui1) are noted. HmK (blue, this work, PDB 6EI7); Hui1 (2N6B, orange); and ShK (4LFQ, grey).

Table S1. Single-particle counting and calculation of effective T-HmK surface concentration. As described in Materials and Methods, T-RFP and T-HmK were expressed in *Xenopus* oocytes by injection of cRNA; single fluorescent particles in 100 μm^2 (n) were counted by smTIRF microscopy; simultaneous photobleaching revealed that all particles contained only one T-RFP (n = 170); average number of T-RFP peptides on the surface of oocytes (N) was estimated based on average surface area; and because the relative surface expression of T-RFP and T-HmK were consistently related (Fig. 1H), the effective concentration of T-HmK could be estimated from the counted number of T-RFP (Fig. 1F) and the measured T-HmK by ELISA (Fig. 1, G and H). With 0.5 ng cRNA injection, the effective concentration of T-HmK is estimated to be 17 ± 2 nM and the K_i of T-HmK block of KcsA-Shaker to be 1.1 ± 0.1 nM, according to Eqn 1. The calculated concentrations of T-HmK with 0.35 and 1 ng cRNA estimated by electrophysiology (F_{un}) are similar to those estimated by ELISA and smTIRF.

T-peptides expressed	Analysis	Determined/Calculated values						
T-RFP	cRNA (ng) injected					0.35	0.5	1
	particles per 100 μm^2 (n)					7 ± 1	16 ± 2	43 ± 5
	number per oocyte (N)					3.5×10^5 ± 0.5×10^5	8.0×10^5 ± 1.0×10^5	2.2×10^6 ± 0.3×10^6
T-HmK	cRNA (ng) injected	0.01	0.05	0.1	0.25	0.35	0.5	1
	F_{un} (fraction unblocked I)	0.98 ± 0.03	0.80 ± 0.07	0.52 ± 0.06	0.24 ± 0.03	0.13 ± 0.01	0.06 ± 0.01	0.025 ± 0.002
	concentration by F_{un} (nM)	0.022 ± 0.003	0.28 ± 0.03	1.0 ± 0.1	3.5 ± 0.4	7.4 ± 0.8	17 ± 2	43 ± 2
	concentration by ELISA (nM)					8 ± 1	17 ± 2	47 ± 5

Table S2. Single-particle counting and calculation of effective T-HmK surface concentration with coexpression of KcsA-Shaker channels.
T-RFP (1 ng) or T-HmK (1 ng) cRNA was injected with or without KcsA-Shaker (1 ng) in *Xenopus* oocytes, single particles counted, and ELISA performed, as described in *Materials and Methods*. The surface concentrations of T-HmK were estimated as described in table S1.

	T-toxin expressed with or without KcsA-Shaker channels					
	T-HmK	**T-RFP**	**T-RFP / T-HmK**	**T-HmK with KcsA-Shaker**	**T-RFP with KcsA-Shaker**	**T-RFP / T-HmK + KcsA-Shaker**
ELISA OD_{450}	0.54 ± 0.01	0.40 ± 0.01	~0.74	0.56 ± 0.01	0.39 ± 0.01	~0.70
RFP particles per 100 μm^2		43 ± 5			41 ± 6	
T-HmK conc estimate (nM)	47 ± 5			49 ± 6		

Table S3. Blocking parameters of hKv1.3 by T-HmK, T-ShK, and the analogous free peptide variants. hKv1.3 inhibition at equilibrium (K_i ± SEM) was determined as described in Figs. 1 and 2; the kinetic parameters were assessed at 0 mV; n = 16-18 oocytes for T-toxins, and n = 6 oocytes for peptides.

Toxins	K_i (nM)	k_{on} (1/Ms)	k_{off} (1/s)
T-HmK	3.0 ± 0.4	$5.4 \times 10^6 \pm 0.8 \times 10^6$	$1.6 \times 10^{-2} \pm 0.2 \times 10^{-3}$
T-HmK-Lys_{22}Asn	702 ± 88	$1.4 \times 10^6 \pm 0.2 \times 10^6$	$9.3 \times 10^{-1} \pm 1.2 \times 10^{-1}$
T-HmK-Arg_{24}Gln	8.1 ± 1.0	$5.3 \times 10^6 \pm 0.8 \times 10^6$	$4.3 \times 10^{-2} \pm 0.6 \times 10^{-3}$
T-ShK	0.098 ± 0.012	$1.2 \times 10^8 \pm 0.2 \times 10^8$	$1.2 \times 10^{-2} \pm 0.2 \times 10^{-2}$
T-ShK-Lys_{22}Asn	0.42 ± 0.05	$7.2 \times 10^7 \pm 0.7 \times 10^7$	$3.1 \times 10^{-2} \pm 0.4 \times 10^{-2}$
T-ShK-Arg_{24}Gln	0.075 ± 0.010	$9.9 \times 10^7 \pm 1.3 \times 10^7$	$7.4 \times 10^{-3} \pm 0.8 \times 10^{-3}$
Peptide HmK	3.1 ± 0.2	$1.1 \times 10^6 \pm 0.1 \times 10^6$	$3.4 \times 10^{-3} \pm 0.2 \times 10^{-3}$
Peptide HmK-Lys_{22}Asn	2225 ± 238	$3.0 \times 10^5 \pm 0.4 \times 10^5$	$6.7 \times 10^{-1} \pm 0.8 \times 10^{-1}$
Peptide ShK	0.05 ± 0.01	$2.7 \times 10^7 \pm 0.4 \times 10^7$	$1.3 \times 10^{-3} \pm 0.1 \times 10^{-3}$
Peptide ShK-Lys_{22}Asn	1.2 ± 0.1	$0.8 \times 10^7 \pm 0.1 \times 10^7$	$9.6 \times 10^{-3} \pm 0.9 \times 10^{-3}$
Peptide ShK-Arg_{24}Gln	0.034 ± 0.006	$2.4 \times 10^7 \pm 0.3 \times 10^7$	$0.8 \times 10^{-3} \pm 0.1 \times 10^{-3}$

Table S4. ^{1}H chemical shifts of HmK. Chemical shifts for HmK (1 mM) ^{1}H nuclei in 20 mM potassium phosphate buffer (pH 6.7) and 100 mM NaCl, determined at 293 K and 16.4 T. ND, not detected.

Residue	$^{1}H^{N}$ [ppm]	H^{α} [ppm]	H^{β} [ppm]	H^{γ} [ppm]	H(others) [ppm]
T2	ND	4.22	4.02	1.15	
C3	9.10	4.70	2.92 / 3.00		
K4	7.88	4.56	1.69 / 1.77	1.08 / 1.28	1.56 / 2.87
D5	8.67	5.07	2.60		
L6	9.23	4.45	1.68	1.75	0.91 / 0.80
I7	7.14	4.80	2.13	1.38 / 0.86	0.88
P8		4.28	1.75 / 1.88	2.07 / 2.38	3.48 / 3.76
V9	8.15	3.57	2.09	0.98 / 1.06	
S10	8.08	4.00	3.80 / 3.87		
E11	8.04	4.18	2.11 / 2.22	2.33	
C12	7.81	4.82	3.16 / 2.78		
T13	6.89	4.14	4.48	1.12	
Q14	8.60	4.09	2.55 / 2.64	ND	
I15	8.15	3.86	1.68	0.79 / 1.38 / 1.14	0.84
R16	7.22	3.70	1.04 / 1.61	1.52 / 1.32	2.752
C17	8.42	4.20	3.02 / 3.12		
R18	7.90	4.13	1.82 / 1.73	1.57	3.05 / 3.13 / 7.40
T19	7.73	4.53	4.29	1.19	2.74 / 2.63
S20	8.07	5.10	4.22 / 3.95		
M21*	ND	4.12	2.00 / 2.10	2.55 / 2.74	2.05
K22*	ND	3.99	1.52 / 1.79	0.87	1.19 / 2.74 / 2.63
Y23	7.53	3.95	2.60 /2.89		7.34 / 6.76
R24	8.44	3.88	1.66 / 2.46	1.49 / 1.40	3.19 / 3.30 / 7.23
L25	8.26	4.43	1.51 / 1.76	1.57	0.90 / 0.84
N26	6.94	5.03	2.87 / 3.05		
L27	8.13	4.12	1.51	1.39	0.68 / 0.25
C28	8.62	5.64	3.11 / 3.21		
R29	8.01	3.81	1.54 / 1.71	1.38 / 1.43	3.17 / 3.36 / 7.11
K30	7.16	4.12	1.25 / 1.77	1.56	1.66 / 2.94
T31	10.97	4.00	3.78	1.23	
C32	8.88	4.75	2.91 / 3.23		
G33	7.78	4.04			
S34	8.82	4.54	3.86 / 3.96		
C35	7.83	4.22	3.03 / 3.23		

Table S5. Heteronuclear chemical shifts of HmK. Heteronuclear chemical shifts for HmK determined as described in Table S4. ND, not detected.

Residue	^{15}N [ppm]	$^{13}C^{\alpha}$ [ppm]	$^{13}C^{\beta}$ [ppm]
T2	ND	62.36	69.76
C3	ND	55.05	38.00
K4	124.37	55.02	ND
D5	121.90	54.53	ND
Y6	120.20	55.00	ND
L7	113.43	58.42	38.58
P8		63.42	ND
K9	122.05	66.03	ND
S10	115.22	59.26	61.97
E11	118.68	56.09	30.62
C12	122.49	51.72	38.00
T13	109.90	60.03	70.24
Q14	121.31	57.84	ND
F15	116.19	63.38	37.78
R16	125.39	60.45	ND
C17	114.80	NA	ND
R18	114.56	NA	ND
T19	105.81	62.55	71.70
S20	116.91	55.92	ND
M 21*	ND	59.00	ND
K22	ND	ND	ND
Y23	117.78	55.52	ND
R24	118.05	ND	31.21
L25	109.93	54.41	ND
N26	114.45	54.85	ND
L27	117.25	58.78	ND
C28	117.18	54.53	ND
K29	117.95	59.95	ND
K30	115.84	58.43	ND
T31	125.20	60.26	68.82
C32	113.53	52.77	35.00
G33	105.80	46.82	
T34	116.18	57.70	63.40
C35	122.90	55.74	63.44

Table S6. Statistics for HmK structure calculation.

NMR distance restraints	
Total inter-residue restraints	212
Sequential ($\|i - j\| = 1$)	124
Medium range ($1 < \|i - j\| < 5$)	51
Long range ($\|i - j\| \geq 5$)	37
NOE violations (Å)	
Maximum single violation	0.5
rmsd of NOE violations	0.071 ± 0.001
Dihedral angle restraints	
Total dihedral restraints	82
Experimental (φ)	10
TALOS derived (φ,ψ)	72
Dihedral angle violations (°)	
Maximum single violation	5
rmsd of dihedral violation	0.86 ± 0.03
Deviation from idealized geometry	
Bond lengths (Å)	0.0022 ±0.0002
Bond angles (°)	0.472 ± 0.004
Improper angles (°)	0.36 ± 0.01
Mean rmsd values (Å)	
Backbone (residues 3-35)	0.31
Heavy atoms (residues 3-35)	1.16